Journal of Computing and Electronic Information Management
ISSN: 2413-1660 | Vol. 19, No. 2, 2025

Dynamic Modeling and Error Mechanism Analysis of a Laboratory Drilling Fluid Automatic Batching System

Anqi Wang, Shenghu Pan

Southwest Petroleum University, Chengdu 610500, China

Abstract: To address the issues of low accuracy in adding trace amounts of powder and the susceptibility of dynamic weighing to disturbances during the preparation of laboratory drilling fluids, this paper conducts an in-depth dynamic modeling and error mechanism analysis of an automatic batching system. First, by analyzing the physical characteristics of the screw feeding mechanism and the resistance strain-gauge load cell, a full-link dynamic mathematical model was constructed, encompassing material flow rate, a second-order weighing system, and the material falling impact force. Next, using a conventional dual-speed feeding strategy as the subject, numerical simulations were performed with Python to quantitatively investigate the effect of the speed switching magnitude (Δn) during the coarse/fine feeding stages on the system's dynamic response. The simulation results indicate that the falling impact force is the primary cause of the weighing system's transient oscillations, and its oscillation amplitude exhibits an approximately linear positive correlation with the speed switching magnitude Δn. The study reveals that to meet the high-precision batching requirement of ±0.01 g, the speed switching magnitude must be strictly constrained. The research outcomes of this paper provide a solid theoretical foundation and key parameter design guidance for the subsequent development of high-precision, high-stability flexible control strategies.

Keywords: Drilling fluid; Automatic batching; Dynamic weighing; Dynamic modeling; Error analysis; Numerical simulation.

1. Introduction

As the "lifeblood" of drilling operations, the performance of drilling fluid directly affects drilling efficiency, cost control, and downhole safety. The accurate reproduction and optimization of drilling fluid formulations in a laboratory environment are fundamental to their successful field application. Traditional manual batching methods suffer from low efficiency, poor repeatability, and susceptibility to human error, making it difficult to ensure formulation accuracy, especially when dealing with trace and multi-component additives. Therefore, the development of high-precision automatic weighing and batching systems has become a key technological trend in this field.

Although automatic weighing and batching systems are widely used in industrial applications, they still face challenges in high-precision laboratory settings (typically requiring accuracy better than ±0.01 g). The core difficulty lies in the precise control of the dynamic weighing process. The process of material falling from the feeding outlet to the weighing hopper generates a significant impact load, causing transient oscillations in the load cell signal [1]. Concurrently, the presence of "in-flight material" (i.e., material that has left the feeding outlet but has not yet reached the hopper when the stop command is issued) is another key factor leading to weighing overshoot. Furthermore, control system response delays, signal conversion errors, and environmental noise collectively constitute a complex web of error sources [2].

Currently, research on compensating for dynamic weighing errors primarily focuses on hardware improvements (e.g., adding buffer devices) and software algorithm optimization (e.g., filtering algorithms, predictive control) [3]. However, most studies emphasize the passive processing of existing signals and lack an in-depth analysis of the system's error generation mechanisms. In particular, fundamental questions such as how feeding strategies (e.g., changes in motor speed) excite system oscillations and how various error sources are coupled have not yet been clearly explained from a dynamics perspective.

In view of this, this paper aims to reveal the intrinsic laws of dynamic weighing errors by establishing a full-chain dynamic model of the system. The main work of this paper includes: (1) establishing an integrated mathematical model that incorporates screw feeding, material impact, and a second-order weighing system; (2) based on the traditional dual-speed control strategy, quantitatively analyzing the impact of the motor speed switching magnitude on the system's oscillation characteristics through numerical simulations; (3) revealing the dominant role of material impact force in the error propagation path and clarifying its intrinsic relationship with control parameters. This research aims to provide a theoretical foundation for designing advanced weighing control strategies, thereby enhancing the accuracy and stability of laboratory automatic batching systems for drilling fluids.

2. System Composition and Mathematical Modeling

2.1. System Composition

The core of the laboratory drilling fluid automatic batching system consists of four main functional modules: the Host PC module, the PLC central control module, the weighing module, and the material feeding module, as shown in the diagram below. The Host PC is responsible for human-machine interaction, data processing, and the computation and execution of control strategies. The PLC central control module executes the control commands from the host, coordinating the work of all modules. The material feeding module, composed of a stepper motor and a screw feeding mechanism, controls the precise dispensing of materials. The weighing module, consisting of a hopper and a load cell, receives the material and collects real-time weight data [4].

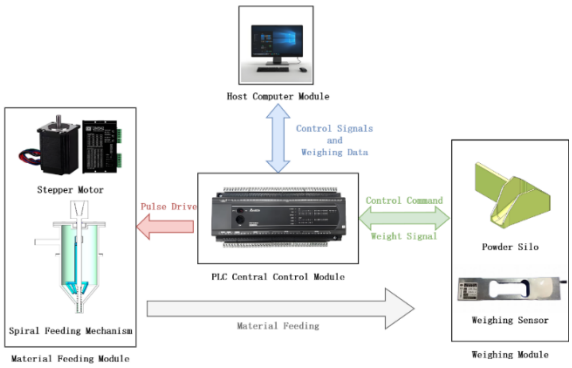

Fig. 1 Schematic Diagram of the Weighing and Batching System Architecture

However, in automatic weighing and batching systems, factors such as material properties, equipment structural characteristics, and environmental interference [5] make it difficult to meet precision requirements. This is typically manifested in the following aspects:

(1) Impact Load of Falling Material

During continuous feeding, the material falling from the feeding device to the weighing unit generates a significant impact load. When the material strikes the weighing hopper at a certain initial velocity, its change in momentum creates a transient overload signal on the sensor's sensitive element. This non-linear impact effect causes mechanical oscillations in the weighing system, leading to distortions in the amplitude-frequency characteristics of the sensor's output signal. This fluctuation often appears as an instantaneous jump in the weight reading, severely affecting weighing accuracy. To mitigate the impact load, a buffer device is often installed above the weighing hopper to reduce the impact force by slowing the material's falling speed. Alternatively, the feeding device's delivery speed can be adjusted, using a lower feeding rate to reduce the impact's kinetic energy.

(2) Effect of In-flight Material

When the control system issues a stop command, there is still material in the space between the feeding device and the weighing hopper that has not fully landed. This suspended material subsequently falls into the hopper, causing the actual weight to exceed the target value, a phenomenon known as overshoot. To address this issue, there are generally two solutions: one is to optimize the mechanical structure to shorten the material's falling distance as much as possible, thereby reducing the amount of in-flight material; the other is to establish a predictive model based on system characteristics to cut off the material supply in advance, thus incorporating the effect of in-flight material into the control strategy.

2.2. Mathematical Model of the Controlled Object

The screw feeding mechanism is the core execution unit for material output in this system, and its flow characteristics directly determine the weighing control accuracy. Therefore, it is necessary to establish a flow rate model for the screw feeding mechanism. Its theoretical flow rate calculation formula is:

$$Q(t)=\frac{\pi}{4}(D-d)^2 Pn(t)K_f\rho C_i\eta \qquad (1)$$

For a specific powder screw feeder, the screw outer diameter D, screw shaft diameter d, pitch P, material filling factor K_f, material bulk density ρ, and inclination correction factor C_i are all constant. In this case, the material flow rate primarily depends on the motor speed n and the material transport efficiency η. For a specific material, its transport efficiency is relatively stable. For different materials, their corresponding transport efficiencies can be determined through experiments. Therefore, it can be considered that the flow rate of the screw feeder is mainly determined by the motor speed n. By dynamically adjusting the motor speed, precise control of the flow rate can be achieved.

Let $C=\frac{\pi}{4}(D-d)^2 PK_f\rho C_i\eta$, the above equation can be simplified to:

$$Q(t)=Cn(t) \qquad (2)$$

The real-time weight in the hopper, $W(t)$, can be obtained by integrating the flow rate:

$$W(t)=\int_0^t Q(\tau)d\tau=C\int_0^t n(\tau)d\tau \qquad (3)$$

2.3. Mathematical Model of the Weighing System

The dynamic quality of the weighing measurement part plays a crucial role in the entire weighing system. A weighing system composed of a resistance strain gauge load cell and a hopper can be simplified as a second-order mass-spring-damper system [6, 7], as shown in Figure 2.

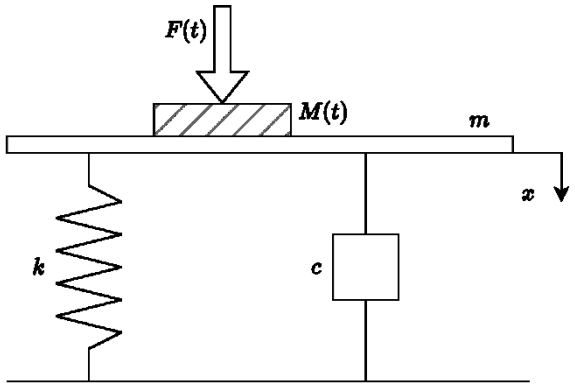

Fig 2 Mathematical Model of the Weighing System

Based on dynamic analysis, the following mathematical model can be established:

$$(m+W(t))\frac{d^2x}{dt^2}+c\frac{dx}{dt}+kx=W(t)g+F(t) \qquad (4)$$

The magnitude of the material impact force $F(t)$ is mainly affected by the material's falling height and velocity. During the coarse feeding phase, the material falls at a faster rate, resulting in a relatively large impact force. In the fine feeding phase, the velocity decreases, and the impact force diminishes accordingly, gradually reducing its effect on the final weighing accuracy. Therefore, the total equivalent input force of the system (including material weight and impact force) can be written as $G(T)=W(t)+F(t)$

The voltage signal output by the load cell is proportional to the deformation x [8]. Thus, equation (4) can also represent the relationship between the sensor's output voltage $U(t)$ and the material weight $W(t)$ .Applying the Laplace transform to equation (4) gives:

$$\Phi(s)=\frac{x(s)}{G(s)}=\frac{\omega_n^2}{s^2+2\zeta\omega_n s+\omega_n^2} \qquad (5)$$

As can be seen from the equation, as the material

continuously falls, $W(t)$ changes, causing the system model parameters ω_n and ζ to decrease accordingly. Thus, the system becomes a time-varying non-linear system. A common simplified analysis method for such systems is piecewise linearization, which assumes that the weight W is constant over a very short time interval $[t, t+\Delta t]$, thereby approximating the system as a second-order linear time-invariant system.

2.4. Modeling of Material Dynamic Characteristics

(1) Estimation of Material Impact Force

According to the momentum theorem, the impact force of a material is caused by a change in momentum and can therefore be expressed by the rate of change of momentum. The calculation formula is:

$$F(t) = \frac{\Delta p}{\Delta t} = Q(t) \cdot V(t) \tag{6}$$

In the formula, the flow rate $Q(t)$ can be calculated from equation (2), so we only need to determine the final velocity $V(t)$. The process of material falling from the outlet to the hopper can be considered as free-fall motion. Based on the uniformly accelerated motion formula, the final velocity can be determined by the initial velocity and the falling height:

$$V(t) = \sqrt{V_0^2(t) + 2gh(t)} \tag{7}$$

The initial velocity $V_0(t)$ can be calculated from the flow rate at the screw outlet:

$$V_0(t) = \frac{Q(t)}{\rho \cdot A} \tag{8}$$

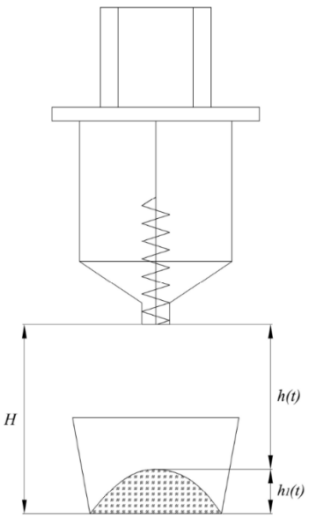

Fig 3 Schematic of Falling Height

The falling height during the dynamic feeding process is shown in Figure 3. Assuming the vertical distance from the feeder outlet to the bottom of the hopper is H, and the height of the powder accumulated in the hopper is h_1. As the feeding process proceeds, h_1 can be calculated by the following formula:

$$h_1(t) = k_h W(t) \tag{9}$$

Then the in-air flight height h of the material is:

$$h(t) = H - h_1(t) = H - k_h W(t) \tag{10}$$

Consequently, the material impact force can be expressed as:

$$F(t) = Cn(t)\sqrt{(\beta n(t))^2 + 2g(H - k_h W(t))} \tag{11}$$

Equation (11) shows that the material impact force is related to the material flow rate and the in-air flight height. The flow rate is controlled by the motor speed $n(t)$, while the in-air flight height is related to the current accumulated weight in the hopper. Since the motor speed appears as a squared term in the formula, its effect on the impact force is much greater than that of the accumulated weight. Therefore, the impact force can be reduced by lowering the motor speed.

(2) Estimation of In-flight Material

It takes a certain amount of time for the material to travel from the outlet to the hopper. When the stop feeding command is issued and the motor stops, some material is still suspended in the air and has not yet landed in the hopper, becoming "in-flight material." The weight of this portion of material will affect the final weighing accuracy, so its weight needs to be calculated to predict the stop command in advance.

Assume the motor speed at the final moment is $n(t)$,then the initial feeding velocity at this time is $V_0(t_z) = \beta n(t_z)$. At this point, the flight time of the powder in the air is Δt. During this time, the weight of the in-flight material, W_{air} , can be expressed as:

$$W_{air} = Q(t_z) \cdot \Delta t = (Cn(t_z)) \cdot \frac{-\beta n(t_z) + \sqrt{(\beta n(t_z))^2 + 2g(H - k_h W(t_z))}}{g} \tag{12}$$

As can be seen from the equation, the weight of the in-flight material at the final moment is related to the motor speed at that time and the weight of the material already in the hopper. The weight of in-flight material decreases as the speed decreases or as the material in the hopper increases, with the motor speed $n(t)$ having the most significant effect. Therefore, in the control strategy, the motor speed at the time of stopping the feed should be as low as possible, and the motor stop timing should be precisely controlled to effectively reduce the weight error caused by in-flight material.

3. Simulation Analysis and Discussion

To investigate the dynamic characteristics of the system, this section conducts numerical simulations based on the traditional two-stage feeding strategy, focusing on analyzing the effect of the speed switching magnitude Δn on the system's response.

3.1. Simulation Setup

The two-stage feeding strategy is a typical phased control method. Its core idea is to divide the entire feeding process into a coarse feeding phase with a large flow rate and a fine feeding phase with a low flow rate. Through a simple and efficient speed switching mechanism, it aims to shorten the feeding time as much as possible while ensuring the accuracy of the target weight. This strategy has the advantages of simple implementation and low hardware requirements, making it widely used in the field of industrial dynamic weighing. In an ideal scenario, the material output and cumulative weight change curves during the traditional two-stage feeding process exhibit distinct two-phase characteristics. Figure 4 shows the weight-time curve and the corresponding motor speed control signal characteristics of this strategy under ideal conditions.

Fig. 4 Speed Control Signal and Weight-Time Characteristics of a Traditional Two-Stage Feeding Process

Furthermore, to deeply analyze the dynamic response characteristics of the traditional two-stage feeding strategy under different motor speed settings, this study designed the following simulation process. This process mainly includes the following steps:

1) Feed Rate and Weight Calculation: Based on screw parameters, calculate the feed rate from the motor speed and obtain the cumulative material weight through integration.
2) Impact Force Calculation: Use the flow rate and motor speed to calculate the material impact force to evaluate its effect on the system.
3) System Response Simulation: Simulate the system's response to input signals (weight, impact force, and total input) based on its transfer function, using the forced response function from the control library.
4) System Oscillation Analysis: Based on the characteristics of the different input curves, select different metrics to analyze the system's oscillations in each phase and calculate system response indicators.

Table 1. Simulation Parameters

Parameter Name	Symbol	Value
Outer Diameter	D	0.012 m
Shaft Diameter	d	0.003 m
Pitch	P	0.006 m
Material Fill Factor	K_f	0.50
Material Density	ρ	1000 kg/m³
Inclination Correction Factor	C_i	0.46
Efficiency Coefficient	η	1.2
Blanking Height	H	0.1 m
Accumulation Factor	K_h	0.1
Weighing Platform Quality	m	0.1 kg
Spring Stiffness	k	1000 N/m
Damping Coefficient	c	0.5 N·s/m
Gravitational Acceleration	g	9.81 m/s²
Time Step	Δt	0.01 s

According to system requirements, the maximum single batch weight is 50 g, so the target weight W_{target} is set to 50 g, and the switching threshold W_{cutoff} is set to $0.9W_{target}$ .Key parameters are shown in Table 1. In the simulation, according to the traditional dual-speed control strategy, the process is divided into coarse and fine feeding phases. Based on actual measurements of the stepper motor used in this system, step loss and abnormal noise occur when n > 10 rps. Therefore, the motor speed for the coarse feeding phase is uniformly set to 10 rps. For the fine feeding phase, five different minimum speeds n_{min} are used: 1 rps, 2 rps, 3 rps, 4 rps, and 5 rps, resulting in 10 combinations of Δn in the two-stage feeding strategy, as shown in Table 2, which can comprehensively cover the motor's speed range.

Table 2. Δn for each phase under five speed combinations

(unit: rps)

n_{min}	Phase One	Phase Two	Phase Three
1	10	9	1
2	10	8	2
3	10	7	3
4	10	6	4
5	10	5	5

3.2. Definition of Evaluation Metrics

To evaluate the system's dynamic performance, two key metrics were defined: Maximum Absolute Error (MaxAE) and Settling Time (t_s). These metrics provide a precise quantitative assessment of the non-linear, time-varying system from the dual perspectives of maximum deviation and the convergence speed of the dynamic process.

Maximum Absolute Error (MaxAE)

MaxAE represents the maximum instantaneous deviation between the actual output and the reference trajectory:

$$\mathrm{MaxAE} = \max_i | y_i - y_{\mathrm{ref},i} | \qquad (13)$$

Where y_i is the output at the i-th sampling point, and $y_{ref,i}$, i is the corresponding reference signal. This metric directly reflects the maximum deviation caused by system oscillations and is a key parameter for evaluating transient response.

Settling Time (t_s)

For the time-varying nature of this non-steady-state system, settling time is chosen as a metric for response speed. It is defined as the time required for the output error to enter and remain within a permissible error band ε from the beginning of a phase. The criterion is:

$$t_s = \max\left\{t_k \mid \exists \delta > T_p : \forall t \in [t_k, t_k + \delta], |e(t)| \le \varepsilon\right\} - t_0 \qquad (14)$$

Where $e(t)$ is the tracking error, $e(t) = y(t) - y_{ref}(t)$; T_p is the system oscillation period, calculated as:

$$T_p = \frac{1}{N-1}\sum_{k=1}^{N-1}(t_{p,k+1} - t_{p,k}) \qquad (15)$$

3.3. Simulation Results and Analysis

(1) Speed Variation Analysis

The speed-time curves for the five speed combinations of the two-stage control strategy are shown in Figure 5, and the flow rates for each phase are listed in Table 3. The simulation results show that the minimum speed of the screw feeder has a significant impact on system performance. In the coarse feeding phase (Phase One), since the maximum speed n_{max}= 10 rps is used, the feed rate remains at a high level of 1.053 g/s. In the fine feeding phase (Phase Two), as the set minimum speed decreases, the feed rate drops significantly. When the minimum speed is reduced to 1 rps, the feed rate is only 0.105 g/s.

Table 3. Feed Rate Q for each phase in five simulations

$n_{\min}$ (rps)	Phase One(g/s)	Phase Two(g/s)	Phase Three(g/s)
1	1.053	0.105	0.000
2	1.053	0.211	0.000
3	1.053	0.316	0.000
4	1.053	0.421	0.000
5	1.053	0.526	0.000

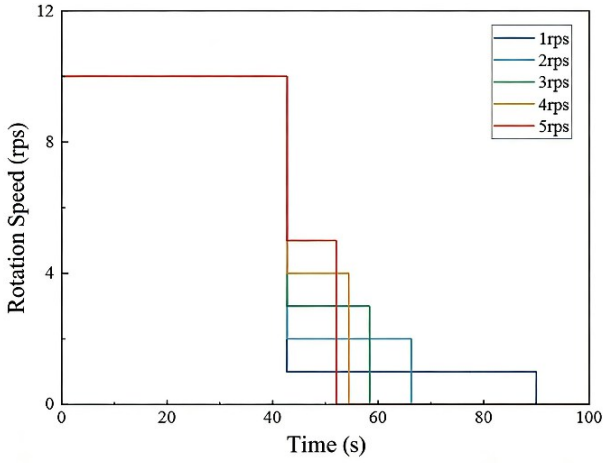

Fig.5 Speed-Time Curves for Different Low-Speed Settings

Under the condition of controlling motor speed with material weight as the independent variable, a lower minimum speed in the fine feeding phase leads to a longer time required to complete this phase. The total feeding time increases from a minimum of approximately t_{min} = 52.08 s to a maximum of approximately t_{max} = 90 s. Therefore, while excessively low parameters can improve accuracy, they significantly increase system operating time. A reasonable minimum speed must be set to achieve a dynamic balance between coarse/fine feeding efficiency and precision.

(2) System Response Analysis

To deeply investigate the effect of the speed switching magnitude Δn on the system's response, the simulated theoretical weight, impact force, and total input signals were separately fed into the second-order oscillating system. Key response metrics, Maximum Oscillation Amplitude (MaxAE) and Settling Time (t_s), were extracted and compiled in Table 4, indexed by Δn.

To more intuitively compare and observe the trends, the metrics from Table 4 were visualized, resulting in the MaxAE bar chart in Figure 6 and the settling time t_s bar chart in Figure 7. The MaxAE of the impact force response (unit: N) was converted to equivalent weight (unit: g) using the formula:

$$W_F = \frac{F}{9.81} \times 1000 \tag{16}$$

Observing Figures 6 and 7, it is evident that as Δn increases, the MaxAE and t_s of all three signals show a consistent upward trend. Specifically, as Δn gradually increases from 1 rps to 10 rps, the MaxAE of the total input signal increases from 0.0137 g to 0.1503 g, and the settling time extends from 0.18 s to 1.61 s. Similarly, the MaxAE and t_s of the theoretical weight and impact force also increase with Δn.

Table 4. System Response Metrics vs. Speed Switching Magnitude

Δn (rps)	MaxAE			Settling Time t_s (s)		
	Weight(g)	Impact(N)	Total Input(g)	Weight	Impact	Total Input
1	0.0013	0.00013	0.0137	0	0.14	0.18
2	0.0026	0.00025	0.0274	0	0.6	0.6
3	0.0038	0.00038	0.0411	0	0.83	0.83
4	0.0051	0.00050	0.0549	0	0.95	0.99
5	0.0063	0.00062	0.0699	0	1.14	1.18
6	0.0073	0.00077	0.0839	0	1.23	1.27
7	0.0086	0.00090	0.0980	0	1.34	1.38
8	0.0099	0.00103	0.1121	0	1.42	1.46
9	0.0112	0.00115	0.1262	0.05	1.46	1.5
10	0.0167	0.00137	0.1503	0.31	1.57	1.61

Further analysis of the data in Table 4 shows that when Δn increases from 5 rps to 10 rps, the MaxAE of the total input signal increases from 0.0699 g to 0.1503 g, an increase of 115.0%. The settling time extends from 1.18 s to 1.61 s, an increase of 36.4%. These data indicate that an increase in Δn significantly degrades the system's dynamic response, not only exacerbating oscillations but also prolonging the settling time.

Comparing Figure 8 (weight response simulation curves for different n_{min}) and Figure 9 (total input response simulation curves for different n_{min}), it can be seen that although both signals show a trend of stabilizing as Δn decreases, there is a clear difference between them. Under the same conditions, the oscillation amplitude of the weight response is much smaller than that of the total input response. When Δn < 9 rps, t_s is 0, achieving instantaneous stability, while the minimum t_s for the total input is 0.18 s. Combined with Figure 6, the equivalent weight of the impact force MaxAE is very close to the total input MaxAE, and their settling times are also quite similar (as shown in Figure 7).

This indicates that the oscillations in the total input signal and its longer settling time are primarily caused by the impact force.

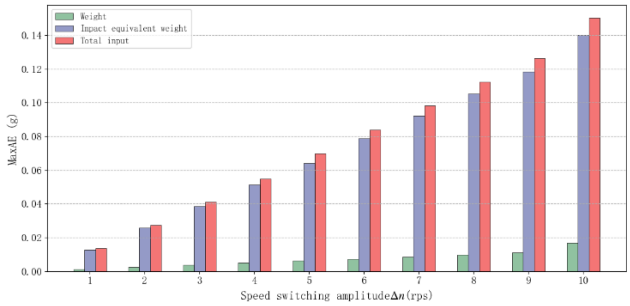

Fig. 6 MaxAE Bar Chart for Different Δn

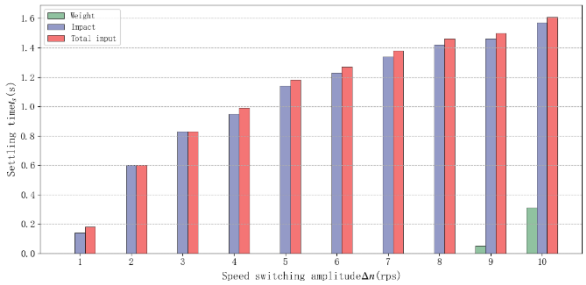

Fig.7 Settling Time t_s Bar Chart for Different Δn

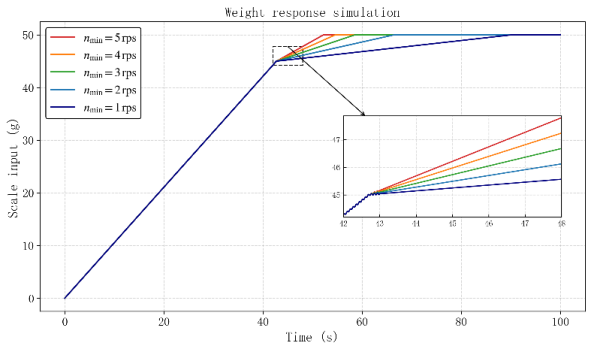

Fig. 8 Weight Response Simulation Curves for Different n_{min}

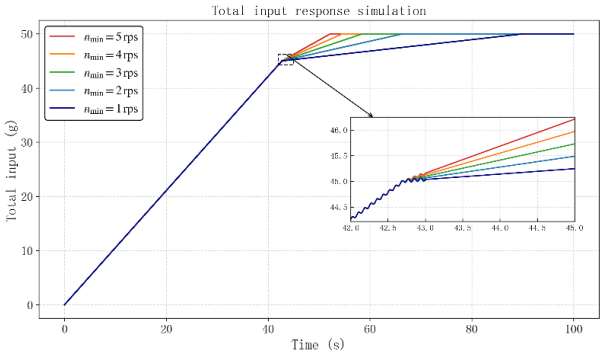

Fig.9 Total Input Response Simulation Curves for Different n_{min}

The data from Table 4 and the analysis of Figures 6, 7, 8, and 9 collectively show that the speed switching magnitude Δn is a key factor affecting the system's dynamic response. Increasing Δn significantly increases system oscillations (especially the oscillations of the total input signal, which are mainly affected by the impact force) and settling time. Conversely, reducing Δn, especially by using a lower minimum speed n_{min} in the fine feeding and stopping phases, can effectively suppress the oscillations caused by the impact force, thereby improving the system's stability and accuracy.

Furthermore, it can be seen from Figure 6 that Δn and MaxAE have an approximately linear relationship. Therefore, to more accurately describe the relationship between Δn and the system oscillations of the total input signal, and to find the maximum Δn that allows the total input MaxAE to be 0.01 g, a linear regression method was used to perform a numerical fit on the simulation data, as shown in Figure 10.

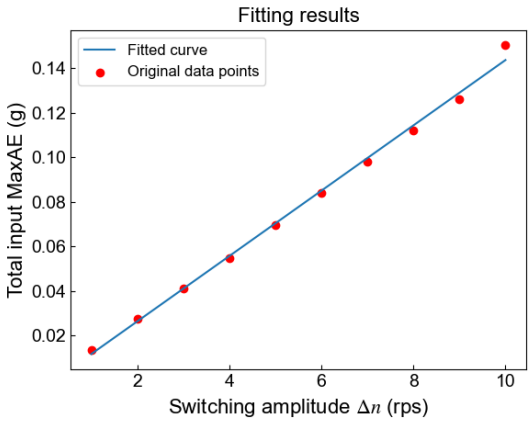

Fig.10 Δn vs. Total Input MaxAE

The mathematical expression for the relationship between Δn and the system oscillation amplitude is as follows:

$$y = 0.014657x - 0.002867 \quad (17)$$

Solving equation (17) in reverse, we can find that when the total input oscillation is 0.01 g, the corresponding Δn is approximately 0.878 rps.

4. Conclusion

Through dynamic modeling and simulation analysis of the laboratory automatic batching system for drilling fluids, this paper has deeply investigated its error generation mechanisms and drawn the following main conclusions:

1) A full-chain dynamic model was successfully constructed: This model integrates the screw feeder flow rate, the dynamic response of a second-order weighing system, and the material impact force, effectively describing the complex behavior of the system during dynamic feeding.
2) The core cause of system oscillations was identified: Simulation results confirm that the step-like change in motor speed, which causes an abrupt change in the material impact force, is the primary reason for transient oscillations in the weighing signal and measurement errors.
3) The relationship between control parameters and system oscillations was quantitatively revealed: The study found that the system oscillation amplitude (MaxAE) has an approximately linear positive correlation with the speed switching magnitude Δn. Based on this relationship, this paper derived a key control constraint to meet the ±0.01 g accuracy requirement: the single-step speed switching magnitude should be less than 0.878 rps.
4) The findings of this study not only explain the origin of dynamic weighing errors from a mechanistic perspective but also provide a quantified theoretical basis and parameter boundaries for the design of high-precision weighing control algorithms. Future work will be based on these conclusions to design and validate a flexible control strategy based on smooth

speed transitions, aiming to achieve higher precision and stability in automatic batching.

References

[1] Chatterjee I, Liao C-F, Davis G 2016 A statistical process control approach using cumulative sum control chart analysis for traffic data quality verification and sensor calibration for weigh-In-motion systems Journal of Intelligent Transportation Systems 21 0–0

[2] Zhang L, Li Q 2023 Dynamic weighing algorithm of bait based on improved strong tracking unscented kalman filtering JOURNAL OF SHANGHAI OCEAN UNIVERSITY 32 967–977

[3] Kang J 2025 High-precision dynamic logistics weighing system based on GRU-BP algorithm Journal of Mechanical & Electrical Engineering 41 1127–1134

[4] Wang Z, Dai Z, Xiang J, Peng J, Zhuang X 2022 Micro high precision weighing system for flocculent powder products Jidian Gongcheng 39 330–336

[5] He H-M, Huang P, Hou D, Cai W, Liu Z, Zhang G 2013 An intelligent signal processing method for high-speed weighing system ijfe 9 179–186

[6] Niedźwiecki M, Meller M, Pietrzak P 2016 System identification based approach to dynamic weighing revisited Mechanical Systems and Signal Processing 80 582–599

[7] Shi H 2013 Measuring and analyzing of static characteristics of vehicle capacitance weighing device Applied Mechanics and Materials 385–386 554–559

[8] Takezawa A, Nishiwaki S, Kitamura M, Silva ECN 2010 Topology optimization for designing strain-gauge load cells Structural and Multidisciplinary Optimization 42 387–402